Pramāṇa – J. Phys., Vol. 31, No. 5, November 1988, pp. 399–412. © Printed in India.

Computer simulation of proton channelling in beryllium

K RAJASEKHARAN* and K NEELAKANDAN+

*Department of Physics, Malabar Christian College, Calicut 673 001, India
+Department of Physics, University of Calicut, Tenhipalam 673 635, India

MS received 3 April 1987; revised 18 July 1988

Abstract. The channelling of protons through a thin beryllium crystal is simulated in a computer. The angular dependence of the momentum density is computed using particle trajectory approximation and is reported as the transmission spectra. In obtaining the spectra, the energy loss suffered by protons due to electron multiple scattering is considered and the effect of thermal vibrations treated separately. The spectra obtained are characteristic of the hcp structure of Be. Positions of the major dips in the transmission spectra are found to correlate well with the directions of neighbouring strings. Variations in the angle of incidence of the beam and in its initial azimuthal angle bring about modifications in the spectra depending on the transverse kinetic energy of the incident particles and the crystalline structure of Be. Thermal vibration of the lattice does not modify the spectra appreciably.

Keywords. Axial channelling; particle trajectory approximation; hcp structure; momentum density; computer simulation; beryllium.

PACS No. 61·80

1. Introduction

The phenomenon of channelling of charged particles in crystalline materials was discovered in the early sixties. Since then, a lot of theoretical and experimental work has been done in the field providing us with information on spatial or momentum density of ions, close encounter yield, energy loss etc. (Thompson 1973). Apart from the intrinsic interest in the basic physics of the phenomenon, channelling has found wide applications in the lattice location of dopant atoms in semiconductors, ion implantation and in the measurement of short nuclear lifetimes. But to our knowledge, all these studies have been confined to cubic crystals.

Ellison *et al* (1978) made use of a particle trajectory approximation (PTA) to compute the angular dependence of the momentum density of axially channelled protons in a silicon crystal. They used the continuum-model approximation with Lindhard's potential, ignoring thermal vibrations and electron multiple scattering. The results thus obtained showed good agreement with experimental data.

Here we present a similar calculation for the hexagonal close-packed structure. As a representative sample we have taken transmission of protons through a thin beryllium single crystal. A possible experimental arrangement to measure the angular distribution of the momentum density of the transmitted beam is shown in figure 1. A

+To whom correspondence should be addressed.

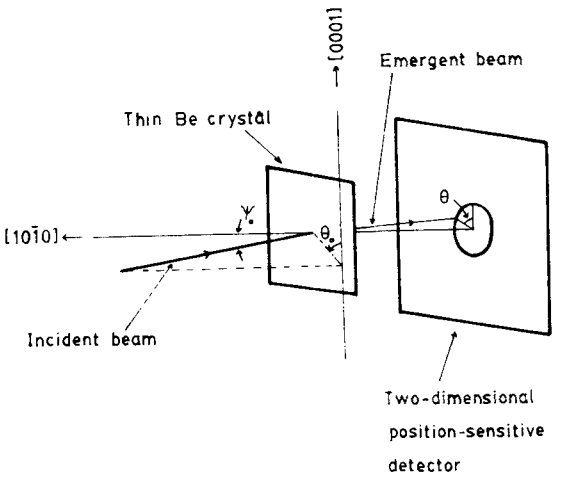

Figure 1. Schematic diagram of an experimental arrangement for measuring the transmission spectra of axially channelled ions in a thin Be crystal.

parallel monoenergetic beam of protons is incident on the crystal at an angle ψ_0 with the $\langle 10\bar{1}0 \rangle$ axis and with an azimuthal angle θ_0 measured about the [0001] axis. The emergent beam is analysed using a two-dimensional position-sensitive detector to obtain the transmission spectra (TS) which give the angular density at various azimuthal angles θ.

This experiment is simulated in a computer using the PTA. We assume zero beam divergence but take into account the energy loss suffered by the particles due to electron multiple scattering. Potentials are determined using the continuum-model approximation. The effect of thermal vibrations is considered separately.

We give the relevant theories in § 2, the method of calculation in § 3 and discuss the results in § 4.

2. Theory

2.1 *Continuum-model*

We consider a proton beam of energy E incident on a single crystal of Be at a small angle ψ_0 with the $\langle 10\bar{1}0 \rangle$ direction. If ψ_0 is chosen to be less than the critical angle ψ_1, a good fraction of the incident ions are channelled within the crystal. We can make use of the continuum-model approximation to describe the motion of an ion inside the crystal. In this model, the chain of atoms in the channelling direction is replaced by a continuum potential string. Since this string potential is independent of the depth z into the crystal, we can describe the motion in a plane transverse to the direction of incidence.

Figure 2 shows this transverse plane. Each black dot represents a string of atoms and the rectangle is a sample unit cell. If a and c are the lattice constants of the hcp structure, the sides of the cell are $a/2$ and $c/2$.

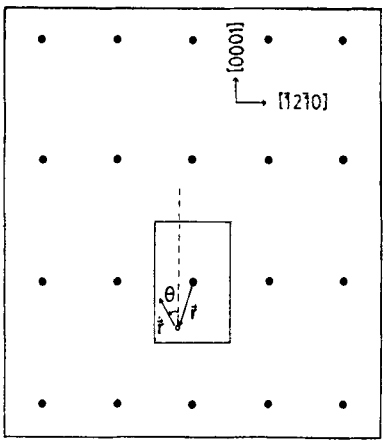

Figure 2. Transverse plane associated with the [10$\bar{1}$0] axis for a Be crystal lattice. The small circle is an ion within the cell and is described by the position vector **r**, velocity vector **ṙ** and azimuthal angle θ.

To describe the motion of an ion, the central string in the unit cell is taken as the origin and the position vector **r** and velocity **ṙ** are defined as

$$\mathbf{r} = x\mathbf{i} + y\mathbf{j}, \tag{1a}$$

and

$$\dot{\mathbf{r}} = \dot{x}\mathbf{i} + \dot{y}\mathbf{j}, \tag{1b}$$

where **i** and **j** are unit vectors in the [$\bar{1}$2$\bar{1}$0] and [0001] directions respectively. The potential $V_s(r)$ due to a single atomic string at a distance r from it is given by Lindhard string potential (Lindhard 1965)

$$V_s(r) = (Z_1 Z_2 e^2/4\pi\varepsilon_0 d)\ln[1 + (C^2 a_T^2/r^2)], \tag{2}$$

where Z_1 and Z_2 are the atomic numbers of the ion and target respectively, e is the electronic charge, d is the average interatomic spacing along the string, C^2 is an adjustable parameter which is usually taken to be 3 and a_T is the Thomas-Fermi screening radius given by the equation

$$a_T = 0{\cdot}8853 a_H (Z_1^{2/3} + Z_2^{2/3})^{-1/2}, \tag{3}$$

where $a_H = 0{\cdot}528$ Å is the Bohr radius. Then $V(\mathbf{r})$, the potential at **r** due to n atomic strings in the transverse plane, is given by the sum

$$V(\mathbf{r}) = \sum_{i=1}^{n} V_s(r_i), \tag{4}$$

r_i being the distance of the point from the ith string.

If M_1 is the mass of the ion, its motion in the transverse plane is governed by Newton's equation, viz.

$$M_1 \frac{d^2\mathbf{r}}{dt^2} = -\left[\frac{\partial V(\mathbf{r})}{\partial x}\mathbf{i} + \frac{\partial V(\mathbf{r})}{\partial y}\mathbf{j}\right]. \tag{5}$$

2.2 *Energy loss*

As the ion traverses the crystal, it loses energy by Coulomb interactions with the nuclei and electrons in the crystal. For protons at MeV energies the energy loss due to nuclear recoils is so small that only the electronic processes need be considered (Poate 1973). The electronic collisions are classified into single particle and resonant collisions. The single particle collisions result in the excitation of individual atoms while the resonant collisions can be identified with the excitation of plasmons in the crystal. Considering both types of collisions, the rate of energy loss is given in terms of the impact parameter because of the varying electron density in the channel, by the formula

$$\frac{dE}{dz}(\mathbf{r}) = -\left(\frac{Z_1^2 e^4}{8\pi\varepsilon_0^2 m v^2}\right)\left(N_c Z_v \ln\left(\frac{2mv^2}{\hbar\omega_p}\right) + \langle N_c Z_c(\mathbf{r})\rangle \ln\left(\frac{2mv^2}{I}\right)\right), \tag{6}$$

as proposed by Bontemps and Fontenille (1978). Here m is the mass of the electron, N_c is the number of atoms per unit volume of the crystal, v is the velocity of the ion, Z_v is the number of valence electrons per atom, ω_p is the plasma frequency and I is the mean excitation energy of the target atoms. $\langle N_c Z_c(\mathbf{r})\rangle$ is the mean electron density near the atomic rows and is obtained through Poisson's equation

$$\nabla^2 V(\mathbf{r}) = Z_1 e^2 \langle N_c Z_c(\mathbf{r})\rangle/\varepsilon_0. \tag{7}$$

Using Lindhard's potential in the above equation, we have

$$\langle N_c Z_c(\mathbf{r})\rangle = \frac{Z_2 C^2 a_T^2}{\pi d} \sum_{i=1}^{n} (C^2 a_T^2 + r_i^2)^{-2}. \tag{8}$$

The equation of motion along the z axis is then

$$M_1\left(\frac{d^2 z}{dt^2}\right) = \frac{dE_z}{dz}(\mathbf{r}) \simeq \frac{dE}{dz}(\mathbf{r}). \tag{9}$$

The approximation holds good for low values of ψ_0.

2.3 *Effect of thermal vibrations*

The displacement of atoms from their equilibrium sites due to thermal vibrations alters the shape of the atomic rows by producing slight curvatures along the string corresponding to the phonon propagation in the crystal. The potential at any point $\mathbf{r}$ in the transverse plane therefore depends on both time and depth into the crystal. Hence an exact analysis of the modifications in the string potential is very difficult. Nevertheless, an averaging procedure as adopted by Andersen and Feldman (1970) can be used. In this procedure an atomic string is assumed to execute a vibration in the transverse plane as a whole with a Gaussian probability function

$$f(\mathbf{r}') = (2\pi\langle u_1^2\rangle)^{-1} \exp(-\mathbf{r}'^2/2\langle u_1^2\rangle), \tag{10}$$

where $\mathbf{r}'$ is the displacement of the string from the equilibrium site at any instant. $\langle u_1^2\rangle$

is the mean square displacement in any direction given by the equation

$$\langle u_1^2 \rangle = \left(\frac{3\hbar^2}{kM_2\Theta_D}\right)\left(\frac{\phi(X_m)}{X_m} + \frac{1}{4}\right). \tag{11}$$

Here k is the Boltzmann's constant, M_2 is the mass of the target atom, Θ_D is the Debye temperature and $X_m = \Theta_D/T$, T being the absolute temperature of the target. $\phi(X_m)$ is the Debye function defined as

$$\phi(X_m) = \int_0^{X_m} \frac{x\,dx}{\exp(x) - 1}. \tag{12}$$

If $\mathbf{F}_s(\mathbf{r})$ is the field at $\mathbf{r}$ due to a static string at the origin, the average field $\langle \mathbf{F}(\mathbf{r}, T) \rangle$ at $\mathbf{r}$ due to the vibrating string is given by convolution of the field $\mathbf{F}_s(\mathbf{r})$ with the displacement probability function $f(\mathbf{r}')$ of the atoms

$$\langle \mathbf{F}(\mathbf{r}, T) \rangle = \int_{-\infty}^{\infty}\int_{-\infty}^{\infty} \mathbf{F}_s(\mathbf{r} - \mathbf{r}')f(\mathbf{r}')\,dx'\,dy'. \tag{13}$$

2.4 *Particle trajectory approximation*

In our simulation experiment, we assumed N protons incident on the cell with a uniform spatial distribution. All particles have an initial angle of incidence ψ_0 with the $[10\bar{1}0]$ axis and an azimuthal angle θ_0 between the transverse momentum vector and the [0001] direction, the angle being measured in the counter-clockwise direction (figure 2). The initial transverse momentum components of the particles are then

$$p_{x_0} = -(2M_1 E\psi_0^2)^{1/2} \sin\theta_0, \tag{14a}$$

and

$$p_{y_0} = (2M_1 E\psi_0^2)^{1/2} \cos\theta_0. \tag{14b}$$

With a knowledge of the initial spatial and momentum coordinates, the trajectory of each proton is calculated up to a desired depth z by numerically integrating the equations of motion. From the calculated values of the exit momenta p_x and p_y for each particle, the exit azimuthal angle θ is calculated using the relation

$$\theta = -\tan^{-1}(p_x/p_y). \tag{15}$$

The number of protons ΔN having an exit angle between $\theta + (\Delta\theta/2)$ and $\theta - (\Delta\theta/2)$ is counted. Then according to PTA, for large N and small $\Delta\theta$, the angular density is

$$\rho_\theta(z, \theta) \simeq \Delta N/(N\Delta\theta). \tag{16}$$

3. Calculation

The lattice constants of Be were taken to be 3·5833 Å and 2·2866 Å (Wyckoff 1963). Then the interatomic spacing d in the $\langle 10\bar{1}0 \rangle$ direction is 3·9605 Å. This direction was chosen so that a simple unit cell could be constructed in the transverse plane satisfying

the translational symmetry requirements. The value of the screening radius a_T calculated using equation (3) is 0·2492 Å.

To determine the trajectory of an ion inside the crystal, the equations of motion were integrated numerically assuming a static lattice but considering the energy loss due to electron multiple scattering. The effect of thermal vibrations was considered separately. The numerical integrations were started by the Runge-Kutta method and continued by Störmer's and Milne's predictor-corrector formulae (Scarborough 1971). For the summation in equation (4), only the central string and 24 neighbouring strings were considered so that the potentials could be determined at different points within the unit cell with an error of less than 1%. To determine the rate of energy loss given by (6), the mean excitation energy of Be atom was taken to be 63 eV (Ziegler 1980) and the plasma frequency ω_p found from the expression

$$\omega_p = (ne^2/m\varepsilon_0)^{1/2}, \tag{17}$$

where n is the electron gas density in the crystal. Substituting $n = N_c Z_v$ in the above equation yields a value of $2{\cdot}801 \times 10^{16}$ Hz for ω_p.

Preliminary estimation of trajectories of 1 MeV protons with $\psi_0 = 0{\cdot}175°$ and $\theta_0 = 0°$ showed that a channelled particle incident close to the string loses energy approximately at the rate of 9 eV/Å near atomic strings and 2 eV/Å at points equidistant from two consecutive atomic strings. At a depth of 1000 Å, its energy was found to be approximately 996 keV. This relatively small loss in the net energy suggested the use of an average value of (dE/dz). This was obtained by defining an average of the mean electron density as

$$\langle N_c Z_c(\mathbf{r})\rangle_{av} = (A)^{-1} \iint_A \langle N_c Z_c(\mathbf{r})\rangle \, dx \, dy, \tag{18}$$

the integration being done over the area A of the unit cell. The above integral equal to $N_c Z_2$ is substituted in (6) to give $(dE/dz)_{av}$. For 1 MeV protons this gives a value of 3·5 eV/Å for the average rate of energy loss.

Sample trajectories were then determined by both methods and the exit energies and exit azimuthal angles were compared. The agreement was within 0·1%. Hence further computations were done using $(dE/dz)_{av}$ thus saving considerable computer time.

Knowing the trajectories of all the ions in the beam, the TS were obtained at different depths for various values of N, $\Delta\theta$, ψ_0 and θ_0.

4. Results and discussion

Comparisons of the TS of 1 MeV protons obtained with $\psi_0 = 0{\cdot}175°$ and $\theta_0 = 0°$ for $N = 1410$ particles and $N = 5640$ particles show that an increase in the number of particles considered increases the accuracy of the spectra. Similarly, on reducing the value of $\Delta\theta$ from 5° to 2°, different structures in the spectra get better defined. Here we give results of the more accurate computations obtained with $N = 5640$ and $\Delta\theta = 2°$. Figure 3 gives the spectra in a three-dimensional like plot beginning from a depth of 100 Å up to a depth of 900 Å at 100 Å interval. The third dimension is the depth into the crystal. The angular density is shown only in the range $0° \leqslant \theta \leqslant 180°$ due to the symmetry of the spectra in the other angular range for $\theta_0 = 0°$.

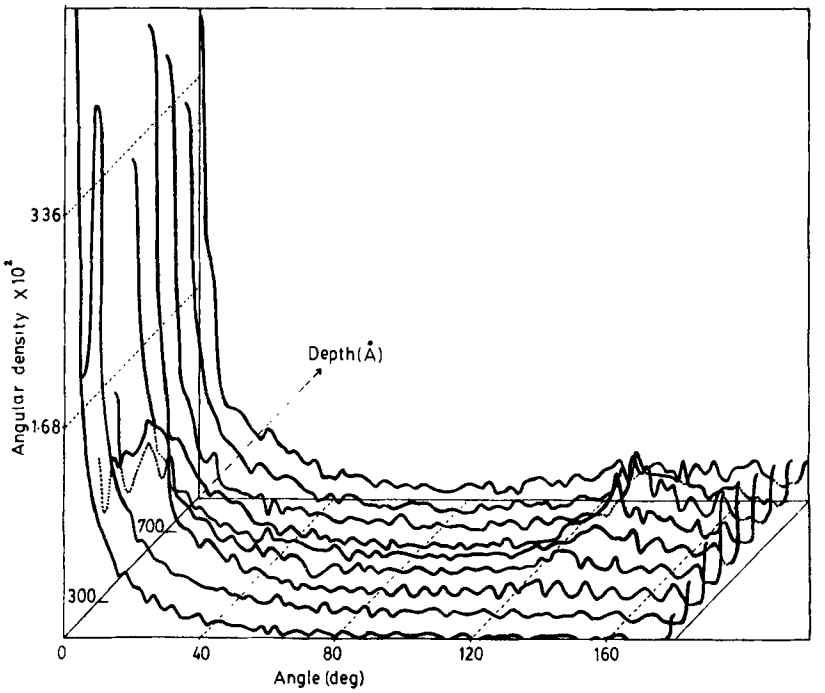

Figure 3. Transmission spectra of 1 MeV protons in Be $(10\bar{1}0)$ with $\psi_0 = 0{\cdot}175°$ and $\theta_0 = 0°$ drawn in a three-dimensional like plot. Parts of the curves which come behind those for lower depths are shown by broken lines.

4.1 *Analysis of the spectra*

For similar spectra in silicon, Ellison *et al* (1978) had found that the positions of major dips coincide with the directions of neighbouring strings from the central string in the unit cell. This correlation was attributed to the collisions of particles with neighbouring strings. The TS obtained from experiments supported their findings.

The spectra of Be could be similarly analysed. We consider some sample trajectories in the plane transverse to $\langle 10\bar{1}0 \rangle$ direction up to a depth of 1000 Å (figure 4). In this figure the paths are numbered near the end-points and their initial positions can be determined by tracing back from the number. Path 1 is for a particle entering the crystal midway between two $\{1\bar{2}10\}$ planes. Due to the symmetric distribution of atomic strings on either side of the entrance position, this particle experiences no field along the $\langle 1\bar{2}10 \rangle$ direction so that its trajectory is straight.

Path 2 resembles planar channelling but cannot be described as one conclusively, since the increasing amplitudes of its oscillations could mean that the path is unstable. All particles entering the crystal midway between the two adjacent $\{1\bar{2}10\}$ atomic planes and in the near vicinity will have paths similar to 1 or 2. They contribute to the peak at 0° in the TS.

Path 3 is for a particle entering the crystal between two adjacent atomic strings lying in the $\{1\bar{2}10\}$ plane. Such particles also do not experience any field in the $\langle 1\bar{2}10 \rangle$ direction as a result of which they execute an oscillation in the $\{1\bar{2}10\}$ plane between the two neighbouring strings as they traverse the crystal. These particles contribute to the peaks at 0° and 180°. As a result of their oscillations, the number of particles moving in

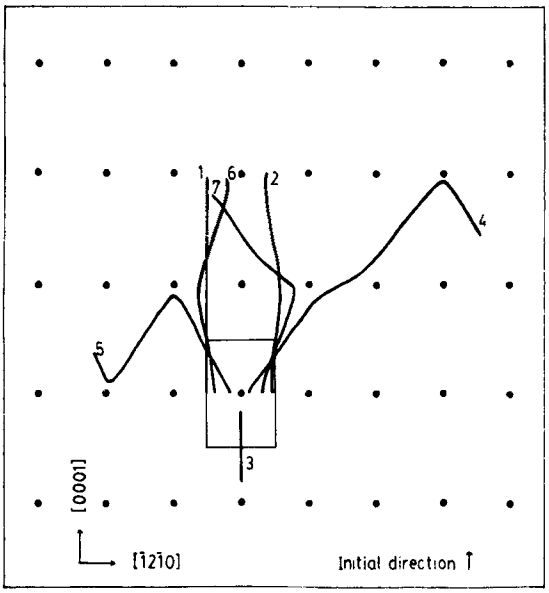

Figure 4. Paths of 1 MeV protons in Be (10$\bar{1}$0) projected in the transverse plane for $\psi_0 = 0{\cdot}175°$ and $\theta_0 = 0°$.

the [0001] or [000$\bar{1}$] direction varies at different depths, causing a fluctuation in the heights of the peaks at these angles.

Paths 4 to 7 show how various particles are deflected off course by the atomic strings. Due to the collisions with the strings and consequent deflections in the trajectories, the number of particles moving in that direction is reduced. Hence we expect the dips in the TS to correspond to the direction of the neighbouring strings. Table 1 gives the distances and directions of neighbouring strings from the central string in the unit cell up to a distance of 6 Å from the central string. The spectra develop a structure around 400 Å after which it is seen that the majority of dips correlate well with the directions of neighbouring strings. Table 2 gives the dips in the spectra which exactly coincide with the directions of neighbouring strings at various depths.

An interesting feature of the spectra is a very prominent peak which starts from a depth of 400 Å at 132° and reaches a maximum at 700 Å moving meanwhile to 138°. An investigation of the trajectories shows that the peak is a result of 72 particles, majority of which start close to the {1$\bar{2}$10} plane. Path 1 in figure 5 is a sample trajectory shown up to a depth of 800 Å. The particle which initially moves along the [0001] direction, suffers a wide angle deflection as it approaches the first string in the {1$\bar{2}$10} plane. It suffers a further deflection but of lesser magnitude by the adjacent string in the same {0001} plane, to proceed at an angle of 138°, thus contributing to the peak at 700 Å. After 700 Å, the particle is gently steered away by an immediate neighbour string, resulting in the disappearance of the peak at the depth of 800 Å.

4.2 *Dependence on the angle of incidence*

Figure 6 shows a comparison of the TS at a depth of 700 Å for the three angles of incidence 0·1°, 0·175° and 0·25°. All the three spectra were obtained for $\theta_0 = 0°$. In

Table 1. Directions and distances of neighbouring strings from the central string.

Distance (Å)	Angle (deg)
1·143	90, 270
1·792	0, 180
2·125	32·5, 147·5, 212·5, 327·5
2·286	90, 270
2·905	51·9, 128·1, 231·9, 308·1
3·429	90, 270
3·583	0, 180
3·761	17·7, 162·3, 197·7, 342·3
3·870	62·4, 117·6, 242·4, 297·6
4·251	32·5, 147·5, 212·5, 327·5
4·572	90, 270
4·912	68·6, 111·4, 248·4, 291·4
4·960	43·7, 136·3, 223·7, 316·3
5·375	0, 180
5·495	12, 168, 192, 348
5·715	90, 270
5·810	51·9, 128·1, 231·9, 308·1
5·841	23, 157, 203, 337
5·991	72·6, 107·4, 252·6, 287·4

Table 2. Directions of neighbouring strings which exactly coincide with the positions of dips in the TS ($\psi_0 = 0{\cdot}175°$, $\theta_0 = 0°$) at various depths.

Depth (Å)	Angle (deg)
400	32·5, 43·7, 68·6, 107·4, 111·4, 128·1, 157
500	17·7, 90, 111·4, 128·1, 157
600	17·7, 23, 32·5, 90, 107·4
700	12, 51·9, 90, 111·4, 147·5
800	62·4, 90, 168
900	17·7, 32·5, 51·9, 72·6
1000	12, 43·7, 111·4, 117·6, 157

addition to the peaks at 0° and 180° it is seen that there is a prominent peak around 138° for all the three spectra. This peak shifts from 128° to 146° when ψ_0 decreases from 0·25° to 0·1°.

To understand this behaviour, we consider a sample trajectory for each value of ψ_0 including path 1 for $\psi_0 = 0{\cdot}175°$ (figure 5). Paths 2 and 3 have ψ_0 of 0·1° and 0·25° respectively and produce peaks at 146° and 128° respectively. From the three paths it can be seen that the prominent peak arises due to a wide angle scattering suffered by a fraction of the particles incident close to the $\{1\bar{2}10\}$ plane. These particles, on entering the crystal, initially move in the [0001] direction; but as they approach the first atomic string in the plane, they suffer wide angle collision. The angle through which the particles are scattered and the position at which the scattering occurs depend on their

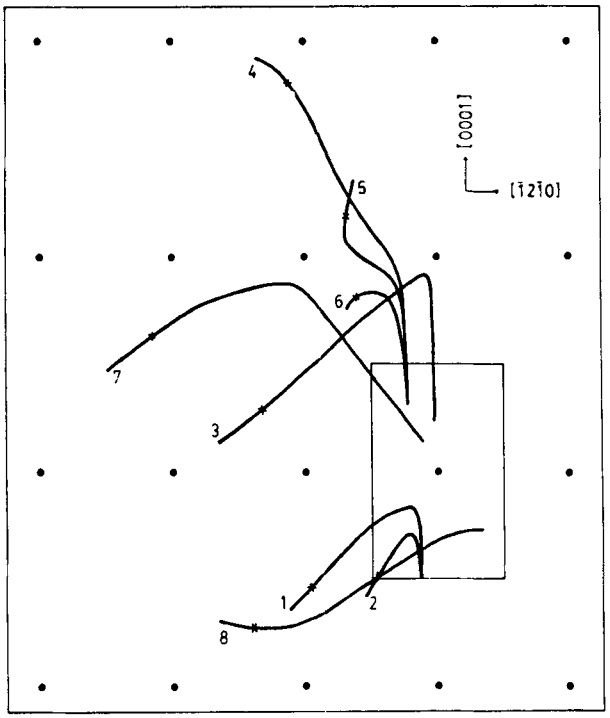

Figure 5. Sample trajectories of 1 MeV protons in Be (10$\bar{1}$0) up to 800 Å. The position of each particle at the depth of 700 Å is shown by a cross.

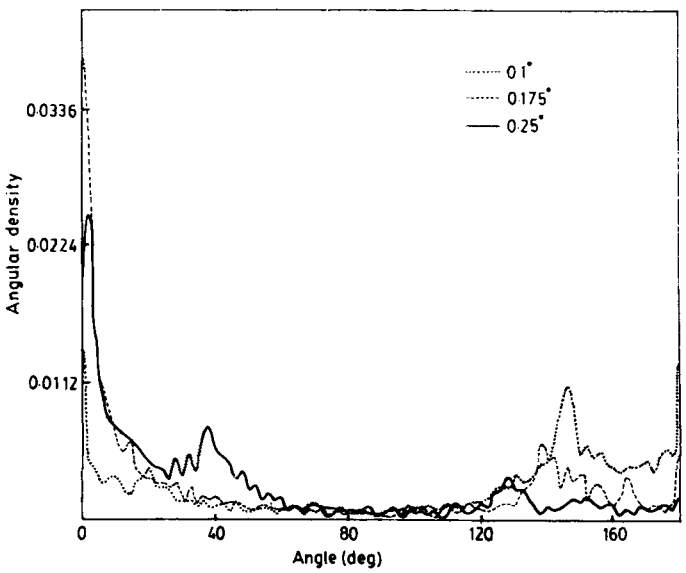

Figure 6. Transmission spectra of 1 MeV protons in Be (10$\bar{1}$0) for three values of ψ_0 compared at a depth of 700 Å. All three of them are for $\theta_0 = 0°$.

transverse kinetic energy (TKE) $E\psi_0^2$. Particles with higher TKE approach closer to the string before they are scattered, the angle of scattering increasing with decreasing TKE. This inverse dependence on TKE can be understood if we consider the scattering of the ion at the string as that due to a central force. It is well known that in such a process the scattering angle is inversely related to the energy of the particle. The angle at which the peak is formed, being approximately equal to the angular deviation suffered, also increases when TKE decreases.

The TS for 0·25° shows another prominent peak at 38° which is not found in the spectra for the other two angles. Path 4 in figure 5 is a sample trajectory with $\psi_0 = 0{\cdot}25°$ producing the peak at 38° at the depth of 700 Å, while paths 5 and 6 are for particles with the same entry point but with ψ_0 values of 0·175° and 0·1° respectively. It is again seen that the difference in the trajectories is due to the difference in their TKE. Paths 5 and 6 have progressively less TKE than that for path 4. Hence at the first encounter with an atomic string in the $\{1\bar{2}10\}$ plane, they are scattered at a wide angle keeping them very close to the $\{0001\}$ plane. As a result, they very soon suffer another close collision with the next string in the $\{0001\}$ plane. On the other hand, for path 4, the angular deviation suffered at the first collision is the least so that it keeps a large distance from the $\{0001\}$ plane. Its trajectory is therefore least influenced by the strings in the $\{0001\}$ plane and it proceeds further to produce the peak at 38°.

4.3 *Dependence on the azimuthal angle*

The TS at a depth of 700 Å for θ_0 values of 0°, 45° and 90° are shown in figure 7. All the curves were obtained for a ψ_0 of 0·175°. The spectra for θ_0 of 0° and 90° can be expected to have some similarities as the particles see an identical distribution of atomic strings

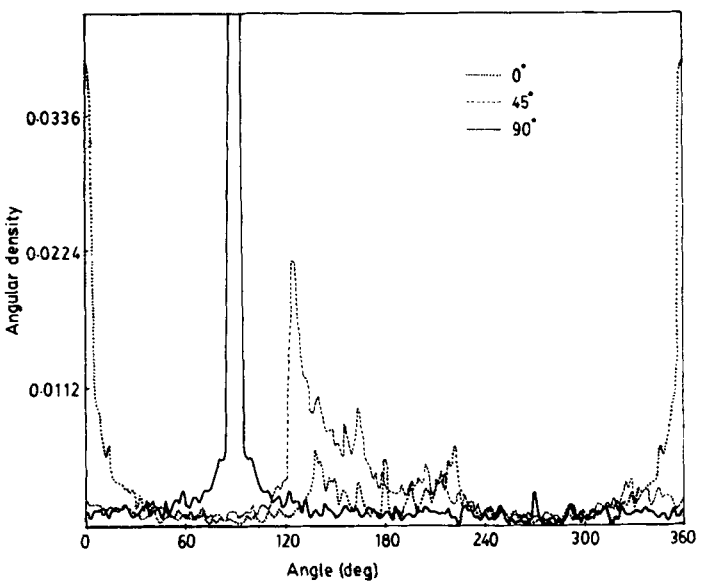

Figure 7. Transmission spectra of 1 MeV protons in Be $(10\bar{1}0)$ compared at a depth of 700 Å for three values of θ_0. $\psi_0 = 0{\cdot}175°$ for all the three curves.

in both cases with the $\{1\bar{2}10\}$ planes changing positions with the $\{0001\}$ planes. Thus instead of the peaks at 0° and 180° in the spectra for $\theta_0 = 0°$, there are peaks at 90° and 270° for $\theta_0 = 90°$. But the spacing between the atomic strings in the $\{1\bar{2}10\}$ plane is more than that in the $\{0001\}$ plane. Therefore a particle incident with its transverse momentum parallel to $\{0001\}$ plane ($\theta_0 = 90°$) encounters more atomic strings in the plane with the result that more particles are likely to undergo planar channelling than when incident parallel to $\{1\bar{2}10\}$ plane ($\theta_0 = 0°$). Hence at certain depths, as at 700 Å, the peak at 90° is very large. Path 8 in figure 5 is a sample trajectory showing this planar channelling. Since the spacing between two adjacent $\{1\bar{2}10\}$ planes is less, the number of particles executing oscillations between two neighbouring strings in the $\{0001\}$ plane is also less. Hence the peak at 270° in the spectra is relatively smaller than the corresponding peak at 180° for $\theta_0 = 0°$.

Path 7 has its initial azimuthal angle equal to 45°. It approaches the $\{0001\}$ plane at a large angle and hence is scattered back into the channel between the two adjacent $\{0001\}$ planes to produce a peak at 126°. A large number of particles have their trajectories similar to path 7 resulting in large angular densities between 120° and 170°.

4.4 *Thermal effects*

The effect of thermal vibration on the TS was studied with $\psi_0 = 0{\cdot}175°$ and $\theta_0 = 0°$. For this, Θ_D in equation (11) was taken to be 1440°K (Kittel 1976) and the strings were assumed to be at 300°K. The TS obtained by assuming a static lattice and that obtained for the thermally vibrating lattice are compared at a depth of 700 Å in figure 8. It is seen that the major peaks in the spectra agree well in their heights and positions. The dips

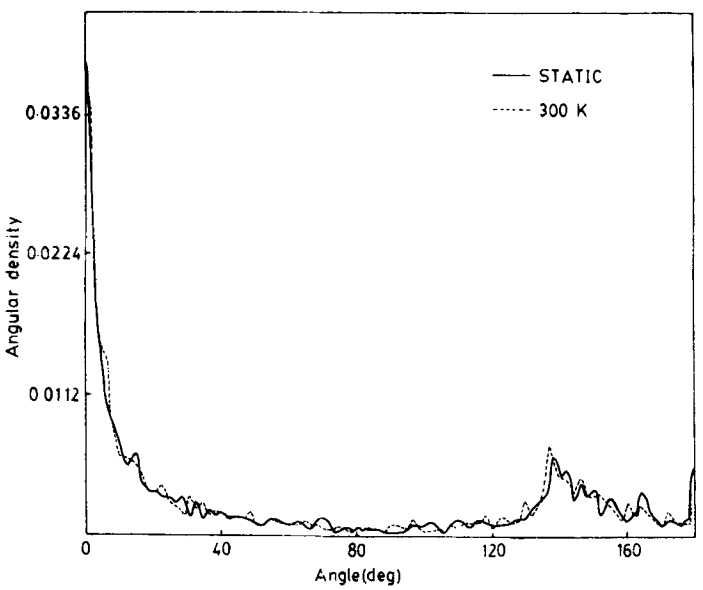

Figure 8. Transmission spectra of 1 MeV protons in Be $(10\bar{1}0)$ with $\psi_0 = 0{\cdot}175°$ and $\theta_0 = 0°$ for a static lattice and a lattice thermally vibrating at 300°K compared at a depth of 700 Å.

also agree in their positions within an error of 2°. On the whole it may be said that the spectra are similar.

Figure 9 shows a plot of average radial field $\langle \mathbf{F}(\mathbf{r}, T) \rangle$ against the distance r from a single $\langle 10\bar{1}0 \rangle$ atomic string at temperatures of 77°K and 300°K, compared with the field due to a static row. It is seen that the difference between the fields due to a string at 300°K and a static string is less than 4% for a distance greater than 0·2 Å from the string. For a distance less than 0·2 Å, the field due to a vibrating string is much less than that due to a static string. In a channelling experiment, only a small fraction of the particles approach the string to a distance of less than 0·2 Å. Hence in majority of the particles there is no appreciable difference between a vibrating string and a static string. The two spectra are, therefore, similar.

5. Conclusions

The TS of protons axially channelled through a thin single crystal of Be in the $\langle 10\bar{1}0 \rangle$ direction were determined numerically using the particle trajectory approximation. The trajectories of protons were obtained using continuum potential accounting for the energy loss due to electron multiple scattering.

The spectra thus obtained are found to be consistent with the hcp structure of Be. Positions of the major dips in the TS correlate well with the directions of neighbouring strings. For an initial azimuthal angle of 0°, two major peaks are obtained at 0° and 180°. The peak at 0° is shown to be the result of planar channelling between the $\{1\bar{2}10\}$ planes while the peak at 180° has been traced to the oscillation of particles between two

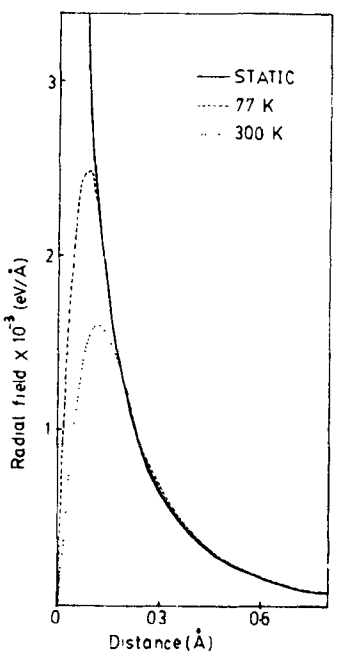

Figure 9. Radial field due to a single $\langle 10\bar{1}0 \rangle$ row of atoms in a Be crystal obtained with and without thermal vibrations of lattice atoms.

neighbouring strings in the $\{1\bar{2}10\}$ plane. At a depth of 700 Å, the spectrum is characterized by a prominent peak around 138°, the exact angle at which it is formed increasing with decreasing TKE of the incident particles.

The TS is also seen to depend on the initial azimuthal angle, with an increase in θ_0 resulting in an increase in planar channelling between the $\{0001\}$ planes.

The effect of thermal vibrations on the TS was studied separately. It is seen that the dependence of the TS on thermal vibrations is negligible.

References

Andersen J U and Feldman L C 1970 *Phys. Rev.* **B1** 2063

Bontemps A and Fonteniile J 1978 *Phys. Rev.* **B18** 6302

Ellison J A, Chui S T and Gibson W M 1978 *Phys. Rev.* **B18** 5963

Kittel C 1976 in *Introduction to solid state physics* (New Delhi: Wiley Eastern) 5th ed., p. 126

Lindhard J 1965 *K. Dan. Vidensk. Selsk. Mat.—Fys. Medd.* **34** No. 14

Poate J M 1973 in *Channelling: theory, observation and applications* (ed.) D V Morgan (New York: Wiley) Ch. 4

Scarborough J B 1971 in *Numerical mathematical analysis* (Calcutta: Oxford & IBH) 6th ed., pp. 363, 348 and 356

Thompson M W 1973 in *Channelling: theory, observation and applications* (ed.) D V Morgan (New York: Wiley) Ch. 1

Wyckoff R W G 1963 *Crystal structures 1* (2nd edn) (New York: Wiley Interscience) Ch. II

Ziegler J F 1980 (ed.) *Handbook of stopping cross-sections for energetic ions in all elements* (New York: Pergamon) Vol. 5 p. 22